

SAR INTERFEROMETRY FOR TOPOGRAPHIC MAPPING AND SURFACE DEFORMATION MONITORING

Urs Wegmüller, Tazio Strozzi, Charles Werner, and Andreas Wiesmann
Gamma Remote Sensing AG
CH- 3074 Muri, Switzerland
<http://www.gamma-rs.ch>, wegmuller@gamma-rs.ch

ABSTRACT

In recent years significant progress has been achieved in repeat-pass spaceborne SAR interferometry. Repeat-pass SAR interferometry combines SAR images acquired over the same area at different times with almost identical sensor positions. The interferometric phase is a measure of the path length difference between the target and the two sensor positions. As a consequence it contains information on the topographic height, surface deformation occurring during the acquisition interval, and path length variations. Under the assumption of a stationary situation (no surface deformation, no propagation effects) the three dimensional position of the image resolution element can be determined, allowing the derivation of terrain height maps. Surface deformation on the other hand may be mapped if the topographic phase term is known from an independent source such as a digital elevation model or an independent interferometric image pair. Examples for surface displacement mapped with SAR interferometry are seismic displacement, land subsidence, land slides, ice motion, and volcano deformation. Under favorable conditions height accuracies of a few meters and sub-cm surface deformation measurement accuracy are feasible.

1. INTRODUCTION

The ERS, JERS, and RADARSAT satellites are the first of a series of spacecraft intended to provide a pre-operational service of ocean, ice, and land observations for the benefit of a large user community. One of the main instruments on board these satellites is a synthetic aperture radar (SAR) imaging the Earth's surface. The development of SAR interferometry has proved that not only the amplitude of the radar signal but also the phase carries valuable information for remote sensing applications. The interferometric phase, that is, the phase difference between two images acquired from slightly different sensor positions, contains "geometric information" allowing the derivation of the three dimensional position of the scatter element. SAR interferometry has developed into an effective technique to generate topographic maps and maps of geophysical surface displacement.

After an overview of the basic methodology of SAR interferometry examples for interferometric height and surface displacement maps will be presented and discussed.

2. METHODOLOGY

Until recently, the phase in SAR imagery was not considered since it is an uniform random variable in the interval $[-\pi, \pi]$ for rough surfaces. However, two images acquired from almost the identical aspect angle, as shown in Figure 1, have almost identical speckle. Under such conditions the phase difference ϕ is related to the imaging path length difference

$$\phi = -\frac{4\pi}{\lambda} (|r_2| - |r_1|), \quad (1)$$

where λ is the radar signal wavelength. The phase is determined as the argument of the normalized interferogram, γ , defined as the normalized complex correlation coefficient of the complex backscatter intensities s_1 and s_2 at positions r_1 and r_2

$$\gamma = \frac{\langle s_2 s_1^* \rangle}{\sqrt{\langle s_1 s_1^* \rangle \langle s_2 s_2^* \rangle}}, \quad (2)$$

with the brackets $\langle x \rangle$ standing for the ensemble average of x . The variance of the estimate of the interferometric phase ϕ is reduced by coherent averaging over a set of looks, which are statistically independent samples of the resolution element. The degree of coherence, a measure of the phase noise, is defined as the magnitude of the normalized interferogram $\gamma = |\gamma|$.

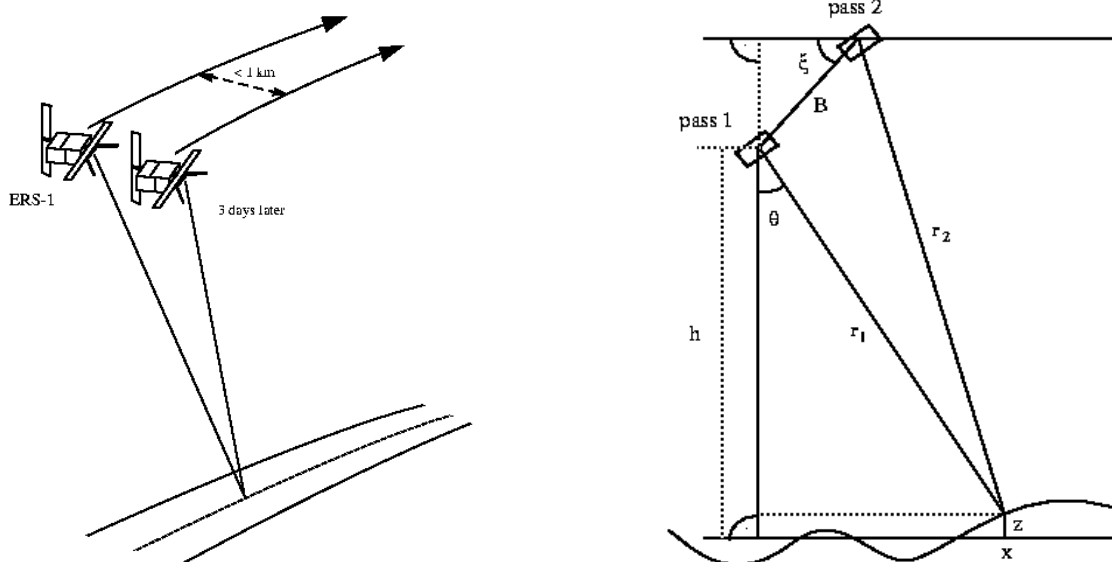


Figure 1: Interferometric imaging geometry showing the two passes with range vectors r_1 and r_2 to the resolution element. The look angle of the radar is θ . The baseline B is tilted at an angle ξ measured relative to horizontal.

The interferometric imaging geometry formed by two passes of a radar sensor separated by the baseline B is shown in Figure 1. The precise look angle θ can be determined from the interferometric phase by solving for the cosine of the angle between the baseline vector and the look vector. The interferometric phase is sensitive to both

surface topography and coherent displacement along the look vector occurring between the acquisition of the interferometric image pair. Inhomogeneous propagation delay ("atmospheric disturbance") and phase noise are the main error sources. The unwrapped interferometric phase ϕ_{unw} can be expressed as a sum of a topographic term ϕ_{topo} , a displacement term ϕ_{disp} , a path delay heterogeneity term ϕ_{path} , and a phase noise (or decorrelation) term ϕ_{noise} :

$$\phi_{unw} = \phi_{topo} + \phi_{disp} + \phi_{path} + \phi_{noise}, \quad (3)$$

and with the expressions for the individual terms introduced:

$$\phi = \frac{4\pi}{\lambda} B_{\parallel} + \frac{4\pi}{\lambda} r_{disp} + \phi_{path} + \phi_{noise}, \quad (4)$$

with the wavelength, λ and the baseline component parallel to the look vector, B_{\parallel} .

Changes in the effective path length between the SAR and the surface elements as a result of changing permittivity of the atmosphere, caused by changes in the atmospheric conditions (mainly water vapor), lead to non-zero ϕ_{path} . The spatial heterogeneity of ϕ_{path} results in the so-called atmospheric distortions, one of the main error sources for in repeat-pass SAR interferometry.

Random (or incoherent) displacement of the scattering centers as well as noise introduced by SAR signal noise is the source of ϕ_{noise} . Multi-looking and filtering of the interferogram reduce phase noise. The main difficulty with high phase noise is not so much the statistical error introduced in the estimation of ϕ_{topo} and ϕ_{disp} but resulting phase unwrapping problems. Ideally, the phase noise and the phase difference between adjacent pixels are both much smaller than π . In reality this is often not the case, especially for areas with a low coherence and rugged topography, as in the case of forested slopes.

The sensitivity of the interferometric phase to the main parameters of interest, i.e. the terrain height (h) and the surface deformation component along radar look vector, r_{disp}) is shown in Table 1 together with characteristic values for the ERS sensor configuration.

Table 1: Interferometric phase terms and characteristic values for the SAR sensors on ERS-1 and ERS-2. The baseline component perpendicular to the radar look vector is B_{\perp} , the incidence angle θ , and the slant range, r , the degree of coherence, γ , and the number of looks used in the phase estimation, N . Notice the very different scale of the effects of the surface topography and deformation.

Phase term	Expression	Characteristic value (for ERS)	Comments
Topographic phase	$\frac{\partial \phi}{\partial h} = \frac{4\pi}{\lambda} \frac{B_{\perp}}{r \sin \theta}$	$\partial h_{2\pi} \approx 100m$ (for $B_{\perp} \approx 150m$)	Ambiguity height is baseline dependent
Deformation phase	$\phi_{disp} = \frac{4\pi}{\lambda} r_{disp}$	$r_{disp,2\pi} \approx 2.8cm$	
Path delay		$ \phi_{path} \leq \pi$	Exceptionally up to $ \phi_{path} > 2\pi$
Phase noise	$stdev(\phi_{noise}) = \frac{\sqrt{1-\gamma^2}}{2N \cdot \gamma}$	$ \phi_{noise} \ll \pi$	For large enough N and non-zero γ .

3. TOPOGRAPHIC MAPPING

Topographic mapping was without doubt the driving idea behind the development of SAR interferometry (see e.g. Graham, 1974, Massonnet et Rabaute, 1993, Madsen et al., 1993, Zebker et al., 1994, Prati et al., 1994). With the availability of repeat track ERS-1 data and the presentation of first very promising results a strong research activity in SAR interferometry started. In the meantime the technique has become more mature and was applied to data of the spaceborne SAR on the ERS-1, ERS-2, JERS, RADARSAT, SIR-C, SEASAT satellites as well as using single and repeat-pass airborne SAR. During the 1995/96 Tandem mission the European Space Agency (ESA) operated its two satellites ERS-1 and ERS-2 in almost identical orbits. With the 1-day acquisition time interval and the short interferometric baselines the Tandem mission was devoted to repeat-pass interferometry. As examples for interferometric height maps Figure 2 shows a height map of North West Rumania, using a gray scale to display the heights, and Figure 3 a shaded relief from interferometric heights for an area in Switzerland. ERS-1/2 Tandem Data were used in both cases. The SAR and interferometric processing as well as the geocoding to ortho-normal coordinates were done using GAMMA's SAR and interferometric processing software (see also <http://www.gamma-rs.ch>).

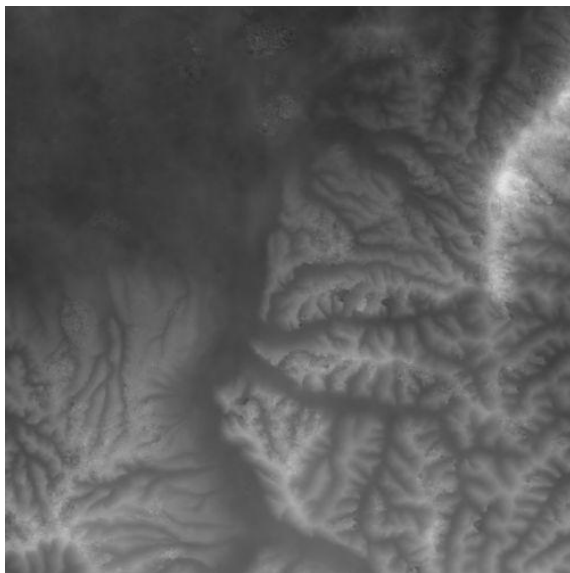


Figure 2: Height map of North West Rumania from ERS-1/2 Tandem data. Area is 40 km x 40 km, a linear gray scale between 0 and 600 m.a.s.l. is used.

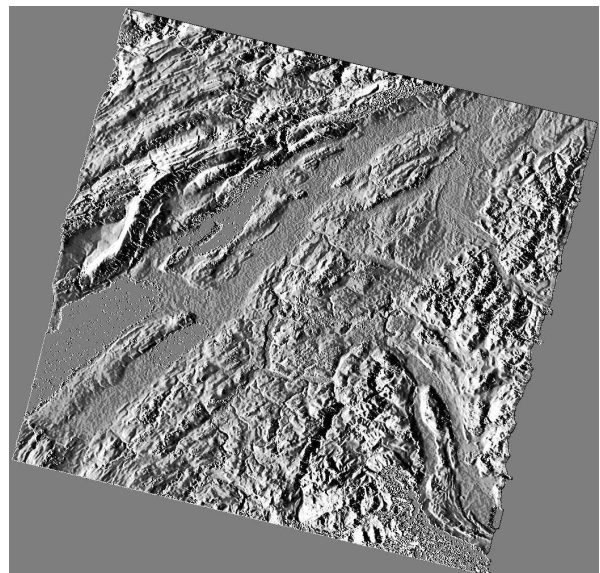


Figure 3: Shaded relief based on interferometric height map for Bern, Switzerland derived from ERS-1/2 Tandem data.

The quality of the interferometric height map depends on several factors. Strong foreshortening and layover occur on slopes tilted towards the SAR causing the scattering of a large surface area with strongly changing terrain height to fall into the same resolution cell. For such areas as well as for radar shadow areas the interferometric phase can usually not be interpreted reliably, resulting in gaps in the interferometric height maps predominantly located on slopes facing towards the SAR look direction. Combining results from ascending and descending acquisitions allows

reduction of this source of error. For areas with coherence below a certain limit the interferometric phase can no longer be interpreted, resulting again in information gaps. For low coherence above this limit the phase noise translates on one hand directly into a height error and on the other hand it may cause phase unwrapping errors. Multi-looking and interferogram filtering allow usually to keep the first error source within an acceptable range. With typical ambiguity heights in the order of 100 m phase unwrapping errors can be a severe problem. The other main error source is atmospheric distortions which are quite frequently up to half a phase cycle for some parts of a frame. Provided that phase unwrapping errors are negligible and that the atmospheric errors are not severe height accuracies of around 5m in relatively flat and 10m in more hilly topography are feasible with ERS Tandem interferometry.

4. GEOPHYSICAL DISPLACEMENT MAPPING

The potential of differential SAR interferometry to map coherent displacement at mm to m resolution resulted in spectacular new results for geophysical sciences. Earthquake displacement [Massonnet et al., 1993], the deformation of volcanoes [Massonnet et al., 1995], the dynamics of glaciers [Goldstein et al., 1993], and land subsidence [Strozzi et al., 1999a, 1999b, Wegmüller et al., 1999] were mapped. The basic idea of differential interferometric processing is to separate the effects surface topography and coherent displacement, allowing to retrieve differential displacement maps. This goal is achieved by subtracting the topography related phase. The topography related phase can either be calculated from a conventional DEM (2-pass approach) or from an independent interferometric pair without or known displacement phase component (multi-pass approach) [Wegmüller et al., 1998].

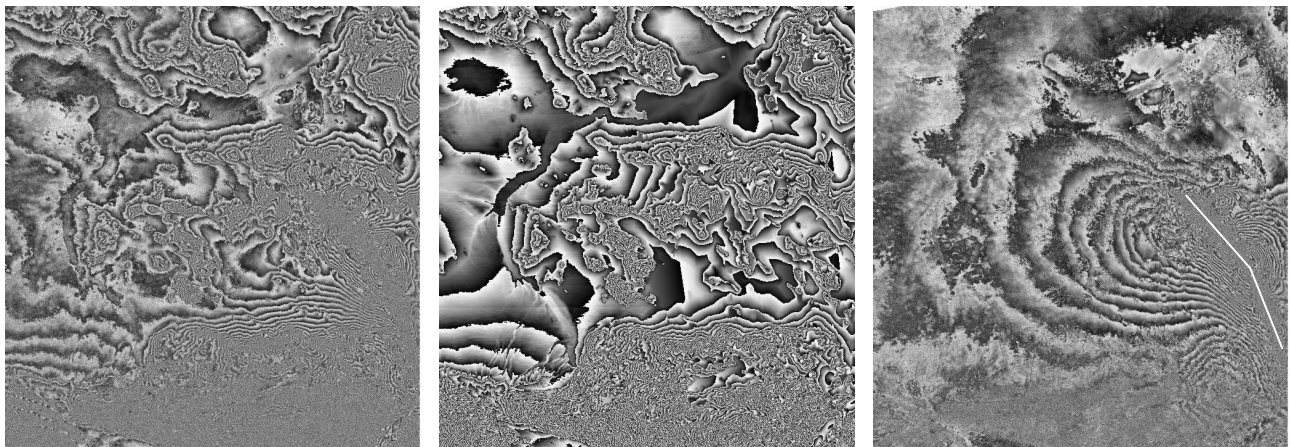


Figure 4: Landers earthquake of June 28, 1992. The left image shows the phase of the flattened interferogram which contains both the topographic and deformation phase terms. The image to the center shows the topographic phase simulated based on a USGS DEM. The right image shows the deformation phase obtained by subtraction of the topographic phase (center) from the interferogram (left image) using the so-called 2-pass approach.

4.1 Seismic displacement

The Landers earthquake occurred on June 28, 1992 in the western USA. ERS-1 SAR acquisitions acquired before and after this event permit derivation of deformation information at cm resolution. Figure 4 shows the interferogram which contains the topographic and the deformation phase terms, the topographic phase term as calculated based on an existing DEM and the differential interferogram obtained by subtraction of this simulated topographic phase from the interferogram using 2-pass differential interferometry. In the resulting image each phase cycle corresponds to a displacement component along the radar look vector of 2.8 cm. The surface can be assumed stable near the left edge of the image. With each phase cycle the total deformation increases. At the main fault rupture, indicated as white line in Figure 4 a displacement of several meters was observed on the ground. Near the rupture the very high fringe density and maybe also to some degree decorrelation from the motion during the earthquake do not allow a direct quantitative interpretation of the interferometric phase.

4.1 Subsidence

Land subsidence in Bologna is caused by ground-water exploitation for industrial, domestic and agricultural uses [Barbarella et al., 1990]. Maximum subsidence velocities of 6 to 8 cm/year were observed with precision leveling surveys between 1987 and 1992. In order to achieve with interferometry the sub-cm accuracy in the subsidence rate estimation necessary to monitor the development of the subsidence rates over time it was necessary to stack multiple independent results using the method described by Strozzi et al., 2000. Two subsidence maps generated for the time periods 1992-1993 (Figure 5) and 1997-1998 (Figure 6) using in both cases six ERS SAR data covering a cumulative time interval of 4 years clearly indicate a decrease of the subsidence rate over this time span. The expected accuracy assuming atmospheric distortions of $\pi/2$ is 0.5 cm/year. The results of differential SAR interferometry are in very good agreement with those derived from leveling surveys (see Strozzi et al., 2000).

Land subsidence of the Euganean Geothermal Basin, Italy, is related to the geothermal groundwater withdrawal. Up to 1991 the maximum rate of land subsidence has been 1 cm/year as observed from precision leveling surveys. After 1991 the subsidence velocity decreased as a consequence of a regulation of the groundwater withdrawal. This example allows to demonstrate the capability of SAR interferometry to map minimal surface displacement with mm accuracy. To map this slow surface displacement a time series of ERS-1 and ERS-2 SAR data from 1992 to 1996 was selected. Multiple interferograms covering in total a time span of more than 20 years were combined into a single displacement map in order to reduce errors caused by atmospheric phase distortions, to a level significantly below the differential phase for the expected slow subsidence. This technique was successful and revealed a clear subsidence signal over Abano Terme with a maximum annual subsidence velocity of 4 *mm/year*, in agreement with the results of the last leveling surveys performed in 1991 and 1995 (Figure 7). The correspondence of the results of the two different surveying techniques is high, as confirmed by a direct quantitative comparison of the interferometry based subsidence values and leveling lines, an example of which is shown in Figure 8. For 17 points where we had values available from both surveying techniques the average difference of the vertical displacement velocity values was 0.2

mm/year with a standard deviation of *1.0 mm/year*. A more detailed description of this case was presented by Strozzi et al., 1999.

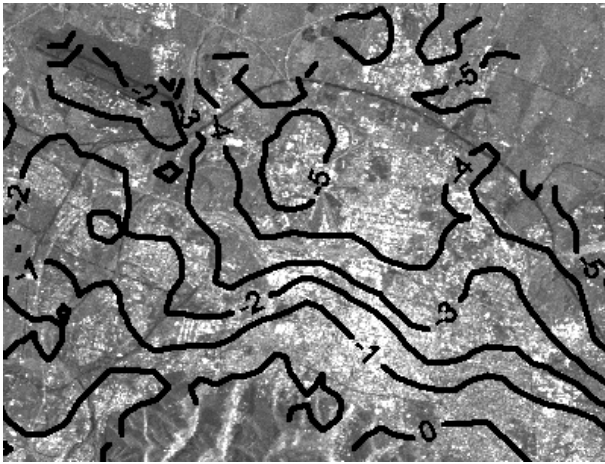


Figure 5: SAR interferometric subsidence map (in *cm/year*) in Bologna for the time period 1992-93.

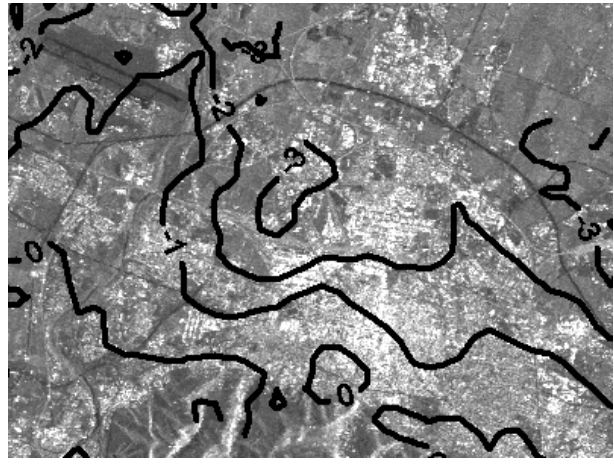


Figure 6: SAR interferometric subsidence map (in *cm/year*) in Bologna for the time period 1997-98.

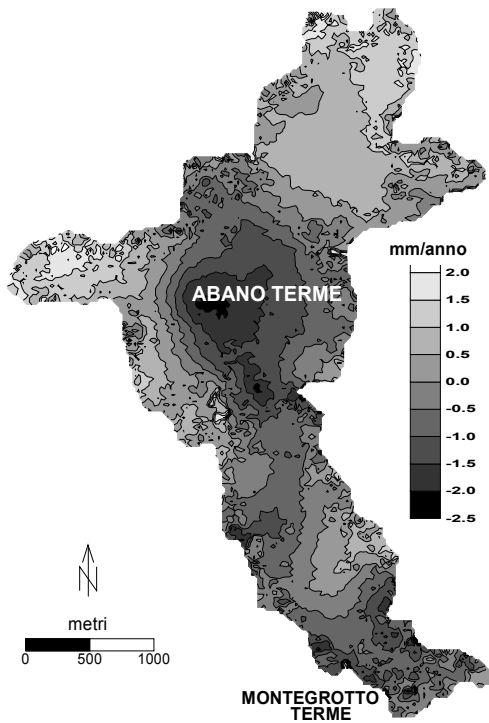


Figure 7. ERS interferometric displacement velocity map (in *mm/year*) for the time interval 1992 and 1996 in the Euganean Geothermal Basin.

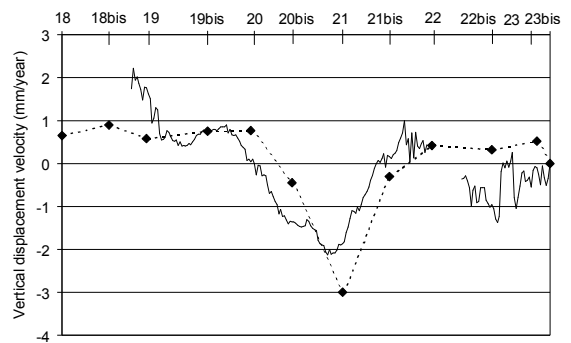


Figure 8. Profiles of the vertical displacement velocity from ERS SAR interferometry (continued line) and leveling surveys (dotted line) along the leveling line Abano Terme – Montegrotto Terme.

5. CONCLUSIONS

The methodology of topographic and surface deformation mapping with repeat-pass spaceborne SAR interferometry was introduced and examples were presented and discussed. The potential and limitations of SAR interferometry for these applications is summarized in Table 2.

Table 2: Potential and limitations of repeat-pass spaceborne SAR interferometry for topographic and surface deformation mapping.

Potential:	Limitations:
<ul style="list-style-type: none">• Topographic height mapping with errors below 10 m in optimal cases.• Land surface deformation mapping with cm accuracy.• Accuracy can be improved by stacking of independent results.• Ascending and descending orbit data can be combined to reduce problems with incomplete coverage and to retrieve two independent displacement components.• Large area coverage (100 km x 100 km).• Relatively high spatial resolution (20 m).• More or less weather independent method.• Daylight independent method.• Existing large data archives with adequate data.• Processing techniques and tools available.• Relatively low cost.	<ul style="list-style-type: none">• Incomplete coverage (strong fore-shortening, layover, radar shadow, low coherence).• Coherence required which limits the applicability for longer acquisition intervals and vegetated areas.• Atmospheric distortion may result in large height errors up to 100 m and large displacement errors up to 2.8 cm.• Phase unwrapping is still a difficult problem to solve. Phase unwrapping errors result in large height or deformation estimation errors.• Only the displacement component along the radar look vector is measured.• Specific requirements concerning baseline and acquisition interval.

6. ACKNOWLEDGMENTS

The Italian National Geologic Survey is acknowledged for the DEMs of the Italian site. Arch. Benetetto Vettore of the Comune di Abano Terme and Ing. Andrea Costantini of the Regione del Veneto are acknowledged for the high precision levelling data used for validation purposes at the Euganean Geothermal Basin. ERS data copyright ESA. ERS data over Rumania courtesy of AO3-175. ERS data over Landers courtesy of AO3-178.

7. REFERENCES

Barbarella M., L. Pieri and P. Russo, "Studio dell'abbassamento del suolo nel territorio bolognese mediante livellazioni ripetute: analisi dei movimenti e considerazioni statistiche", INARCOS 506, 1990.

- Goldstein R. M., R. Engelhardt, B. Kamb, R. Frolich, "Satellite Radar Interferometry for Monitoring Ice Sheet Motion: Application to an Antarctic Ice Stream" *Science* Vol. 262, pp. 1525-1530, 3-dec-1993.
- Graham L.C., Synthetic interferometer radar for topographic mapping, *Proc. Inst. Electron. Engrs*, 62, p 763, 1974.
- Madsen S.N. H.A. Zebker, and J. Martin, Topographic mapping using radar interferometry: Processing techniques, *IEEE Trans. Geosci. Remote Sensing*, Vol. 31, No. 1, pp. 246-256, 1993.
- Massonnet D. and T. Rabaute, Radar interferometry: limits and potential, *IEEE Trans. Geosci. Remote Sensing*, Vol., 31, No. 2, pp. 455-464, 1993.
- Massonnet D., M. Rossi, C. Carmona, F. Adragna, G. Peltzer, K. Feigl, and T. Rabaute, The displacement field of the Landers earthquake mapped by SAR interferometry, *Nature* 364, No. 6433, pp. 138-142, 1993.
- Massonnet, D., P. Briole, and A. Arnaud (1995) Deflation of Mount Etna monitored by spaceborne radar interferometry, *Nature*, vol 375, pp. 567-570.
- Prati C., F. Rocca, and A. Monti-Guarnieri, SAR interferometry experiments with ERS-1, *IEEE Trans. Geosci. Remote Sensing*, Vol. 32, No. 4, 1994.
- Strozzi T., L. Tosi, L. Carbognin, U. Wegmüller, and A. Galgaro, Monitoring Land Subsidence in the Euganean Geothermal Basin with Differential SAR Interferometry, *Proceedings of Fringe'99, Liège (B)*, 1999a.
- Strozzi T. and U. Wegmüller, Land Subsidence in Mexico City Mapped by ERS Differential SAR Interferometry, *Proceedings of IGARSS'99, Hamburg*, 28 June - 2 July 1999b.
- Strozzi T., U. Wegmüller, C. Werner, and A. Wiesmann, Measurement of slow uniform surface displacement with mm/year accuracy, *Proc. of IGARSS'00, Honolulu, USA*, 24-28 July 2000.
- Wegmüller U. and T. Strozzi, Validation of ERS Differential SAR Interferometry for Land Subsidence Mapping: the Bologna Case Study, *Proceedings of IGARSS'99, Hamburg*, 28 June - 2 July 1999.
- Wegmüller U., and T. Strozzi, Characterization of differential interferometry approaches, *EUSAR'98*, 25-27 May, Friedrichshafen, Germany, VDE-Verlag, ISBN 3-8007-2359-X, pp. 237-240, 1998.
- Zebker H.A., C. L. Werner, P.A. Rosen, and S. Hensley, Accuracy of topographic maps derived from ERS-1 interferometric SAR, *IEEE Trans. Geosci. Remote Sensing*, Vol., 32, No. 4, pp. 823-836, 1994.